An X-ray and MIR perspective on AGN unification

F.J. Carrera, P. Fernández-Manteca, and S. Mateos

Instituto de Física de Cantabria (CSIC-UC), Santander, Spain

Abstract

We have investigated the claimed flattening of the X-ray to mid-IR luminosity correlation using the SDSS DR12 QSO sample, correlating it with the XMM DR5 catalogue and UN-WISE, to build a large sample of luminous optically-selected type 1 AGN with measured X-ray and mid-IR luminosities (or upper limits to them).

We confirm that there is a $> 99.9\%$ significant flattening in the correlation, in the sense that the X-ray luminosity "saturates" at the highest mid-IR luminosities. Further work using a direct estimate of the seed optical-UV power will allow discriminating between different explanations for this phenomenon. It may occur because the X-ray generating mechanism cannot keep up with the increase in AGN power, or because the structure of the material reprocessing the primary emission into the mid-IR changes its properties.

1 Introduction

Active Galactic Nuclei (AGN) are the most luminous persistent sources in the Universe, particularly those with the highest luminosities, called QSOs.

The stupendous radiation from AGN would be ultimately powered by accretion into a Super Massive Black Hole (SMBH) through a flattened accretion disk (AD). The hottest central regions of the AD are responsible for the primary UV/optical radiation, seen as the intrinsically blue continuum of AGN [14]. Close to the centre of that disk there is a corona of hot electrons which up-scatter that primary radiation giving rise to the observed X-ray emission from AGN [4]. Finally, another flattened structure, called the central torus, obscures the central engine from direct observation in directions close to the equator, while allowing a free view from polar perspectives. This torus would also be responsible for the strong mid-infrared (MIR) radiation detected from AGN, which is thought to be due to thermal radiation from the obscuring material warmed by the nuclear radiation (reprocessing)[10].

The bewildering variety of AGN properties has been successfully explained with the Unified Model (UM) [1, 11] which, to first order, assumes that all AGN share the same intrinsic structure outlined above, while most of the observed differences coming from the
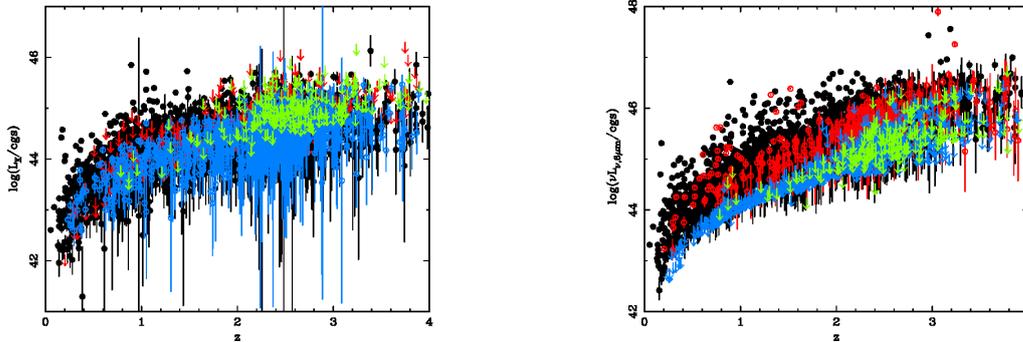
Figure 1: X-ray (left) and MIR (right) luminosity versus redshift for the QSOs in our sample. The individual QSO are colour-coded according to the band(s) in which they are detected: black filled dots if they are detected in both bands, red if they are detected in MIR but not in X-ray, blue if they are detected in X-ray but not in MIR and green if they are undetected in both bands. Round symbols are used for detections and down-pointing arrows for upper limits.

inclination of the symmetry axis of the structure to the line of sight. In this framework, the X-ray and MIR luminosities should be strongly correlated, since both arise from the primary optical/UV radiation from the AD.

This has indeed been observed in the past, both in MIR-driven [8] and X-ray selected samples [9]. However, there have been some recent claims [16] that this relation flattens at the highest MIR luminosities ($\nu L_{\nu,6\mu m} > 10^{43} \, \mathrm{erg \, s^{-1}}$), as if the reprocessed radiation keeps increasing while the X-rays "saturate". This would be very surprising within the UM which, if anything, would expect the obscuring structure to "shrink" under the onslaught of the increasing central luminosity ("receding torus" [15]). However, the flattening observed by Stern15 is mostly driven by about 22 high MIR luminosity objects.

We have constructed a large sample of luminous AGN (QSO) with measured (or constrained) X-ray and MIR luminosities, to investigate the relation between them at the higher end of the distribution and to assess the significance of the flattening, if observed.

2 Our sample

Our aim was to construct a sample of luminous QSO with both X-ray and MIR measurements as large as possible. To this end we have resorted to the largest available samples of sources in those bands, selecting the QSOs using the largest optical spectroscopic sample of such sources.

We have used the SDSS DR12 QSO sample [12] which, by construction, already selects luminous AGN. We have further demanded that they have no other SDSS DR12 photometric source within 5 arcsec, to avoid confusion issues in X-rays (see below), and that their Galactic

latitude $|b| > 20°$, to avoid strong Galactic absorption and obscuration. We have set a quality filter in their redshifts z, also setting a limit of $z < 4$ to improve the quality of the estimated MIR luminosities (see below). Finally, in order to ensure that we have a ~polar view of the central engine, we have asked for $FWHM > 1500\,\mathrm{km\,s^{-1}}$ (where FWHM stands for the Full Width at Half Maximum of the CIV, CIII] or MgII emission lines in their observed optical spectrum), since the Broad Line Region from which those lines come is close to the central engine and would also be obscured by the torus.

We have then selected the subset of those filtered QSO that are under the footprint of the 3XMM DR5 [13] catalogue of serendipitous X-ray sources detected by XMM-Newton [5]. To be precise, we have used FLIX[1] to find the pn [17] exposure time at the position of the QSO above, keeping only those with 5 ks or longer exposures. If more than one XMM-Newton observations covered the QSO, we chose the one with the longest pn exposure. We have then cross-correlated the SDSS DR12 QSO positions with the 3XMM DR5 catalogue positions within 5 arcsec, labelling as X-ray detected those QSOs with a counterpart within that distance. For the X-ray undetected objects, we used the upper limit to the flux in the 2–12 keV band as estimated by FLIX, extracting the counts in a 6 arcsec circle around the SDSS position. These fluxes are converted to rest-frame 2–10 keV luminosities assuming a photon index of 1.4 and the redshifts from SDSS.

Table 1: Number of SDSS DR12 QSO in our sample with detections in each band

	Xdet	Xundet	Total
MIRdet	2451	340	2791
MIRundet	841	218	1059
Total	3292	558	3850

UNWISE [7] provides forced photometry from AllWISE [3] at the positions of the SDSS DR9 photometric sources. We have used the W2 ($\sim 4.6\,\mu\mathrm{m}$) and W3 ($\sim 12\,\mu\mathrm{m}$) fluxes to estimate the monochromatic $\nu L_{\nu,6\mu\mathrm{m}}$ luminosities, interpolating and extrapolating when necessary. If any of those two fluxes is detected at less than 1–σ, the source is flagged as undetected in the MIR band.

We have a total of 3850 QSOs, we provide the subsets according to their detections in the X-ray/MIR in Table 1, and the X-ray and MIR luminosity versus redshift plots are shown in Fig. 1.

3   Results

We show in Fig. 2 L_X versus $\nu L_{\nu,6\mu\mathrm{m}}$ (in log-log) for our full sample (left) and only for the detections (for clarity, right), along with the best fit linear model from [9] (orange) and parabolic model from [16]: it is visually clear that the linear model skims trough the top of the distribution while the parabolic model appears to follow the distribution. To quantify

---

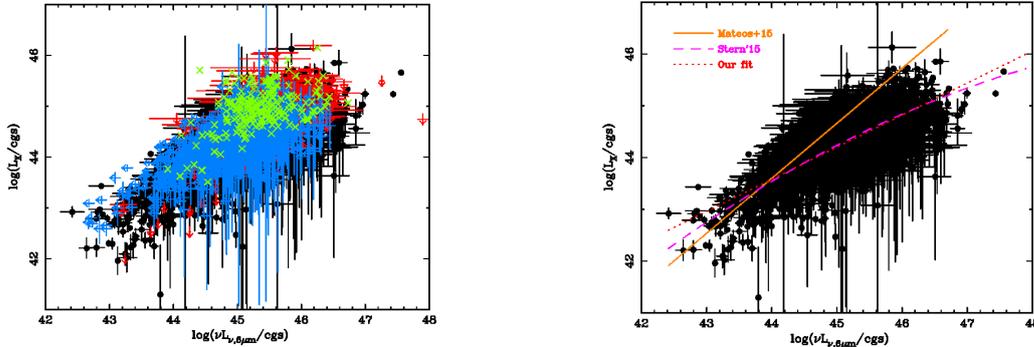[1]http://www.ledas.ac.uk/flix/flix_dr5.html

Figure 2: X-ray versus MIR luminosity of the QSO in our sample. Left: SDSS DR12 QSO detected in both bands (black filled dots), QSOs detected in MIR but not in X-rays (red-down pointing arrows), QSOs detected in X-ray but not in MIR (blue left-pointing arrows) and QSOs undetected in both bands (green "×" signs).

this impression, we have fitted a linear (in log-log) model to our sources detected both in X-rays and in MIR, taking into account the errors in both dimensions, allowing as well for an intrinsic dispersion in the MIR luminosity. The best fit linear slope (exponent in a power-law) is 0.620 ± 0.011 compared to the best fit slope of [9] of 0.94 ± 0.04. The uncertainty in our best fit slope was obtained from 10000 bootstrap simulations, and none of them was as high as the one in [9], which means that the flattening is significant at more then 99.9%.

We thus confirm that the higher MIR luminosity objects appear to be X-ray underluminous, compared with those at lower luminosities.

4   Discussion and conclusions

There are three main caveats to our results:

- Optically-selected BAL QSOs are generally X-ray underluminous for their optical luminosity, so they might also be underluminous for their MIR luminosity. We are planning to exlude BAL QSOs from the sample

- Part of the MIR emission in Radio Loud (RL) QSOs might be related to the jet expected to be present in these sources, so we might be overestimating their MIR luminosities. We will cross-correlate our sample with FIRST [2] to evaluate the impact of RL QSOs

- The fraction of undetected sources is high $\sim 1/3$ of the total sample. Given the distribution of upper limits, it is unlikely to affect strongly the significant flattening that we have observed. We will repeat our fits using the Bayesian technique of [6], which also takes into account errors in both coordinates, intrinsic dispersion and upper limits

Conceding the caveats above, our preliminary results suggest that the X-ray luminosity of QSOs somehow "saturates" at the highest MIR luminosities. Our next step will be to estimate the rest-frame optical/UV luminosities of these objects and compare it with the X-ray and MIR ones that we have obtained above.

If the optical/UV luminosity also flattens for the highest MIR luminosities, since the latter is reprocessed from the former, we would deduce that at the highest luminosites a change of the structure of the torus would happen, so that it somehow becomes more efficient in reprocessing the input optical/UV radiation.

If instead the optical/UV luminosity keeps increasing with increasing MIR luminosity, it would appear that the AD corona cannot reprocess all the input optical/UV radiation, so that the X-ray luminosity "saturates" as observed.

Acknowledgments

References

[1] Antonucci, R., 1993, ARA&A, 31, 473

[2] Becker, R. H., White, R. L., Helfand, D. J. 1995, ApJ, 450, 559

[3] Cutri, R.M., et al., 2013, Technical Report, Explanatory Supplement to the AllWISE Data Release Products

[4] Haardt, F., Maraschi, L., 1991, ApJL, 380, L51

[5] Jansen, F., Lumb, D., Altieri, B., et al. 2001, A&A, 365, L1

[6] Kelly B. C., 2007, ApJ, 665, 1489

[7] Lang, D., Hogg, D.W., Schlegel, D.J., 2014, AnJ, 151, 2

[8] Lutz, D., Maiolino, R., Spoon, H. W. W., Moorwood, A. F. M., 2004, A&A, 418, 465

[9] Mateos, S., Carrera, F.J., Alonso-Herrero, A., Rovilos, E., et al., 2015, MNRAS, 449, 1422

[10] Mor, R., Netzer, H., Elitzur, M., 2009, ApJ, 705, 298

[11] Netzer, H., 2015, ARA&A, 53, 365

[12] Pâris, I., et al., 2016, A&A, submitted

[13] Rosen, S.R., et al., 2016, A&A, 590, A1

[14] Shakura, N. I., Sunyaev, R. A., 1973, A&A, 24, 337

[15] Simpson C., 2005, MNRAS, 360, 565

[16] Stern, D., 2015, ApJ, 807, 129

[17] Struder, L., Briel, U., Dennerl, K., et al. 2001, A&A, 365, L18